

Squeezed Light from Entangled Nonidentical Emitters via Nanophotonic Environments

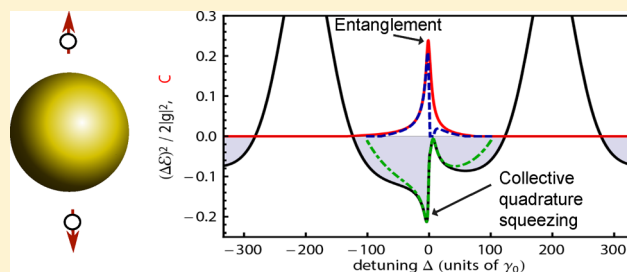
Harald R. Haakh* and Diego Martín-Cano*

Max Planck Institute for the Science of Light, Günther-Scharowski-Straße 1/24, D-91058 Erlangen, Germany

S Supporting Information

ABSTRACT: We propose a scheme in which broadband nanostructures allow for an enhanced two-photon nonlinearity that generates squeezed light from far-detuned quantum emitters via collective resonance fluorescence. To illustrate the proposal, we consider a pair of two-level emitters detuned by 400 line widths that are coupled by a plasmonic nanosphere. It is shown that the reduced fluctuations of the electromagnetic field arising from the interaction between the emitters provide a means to detect their entanglement. Due to the near-field enhancement in the proposed hybrid systems, these nonclassical effects can be encountered outside both the extremely close separations limiting the observation in free space and narrow frequency bands in high- Q cavities. Our approach permits overcoming the fundamental limitations to the generation of squeezed light from noninteracting single emitters and is more robust against phase decoherence induced by the environment.

KEYWORDS: quadrature squeezing, collective resonance fluorescence, entanglement, nanostructures, dipole–dipole coupling, plasmonics



The generation of entanglement, one of the most interesting and nonintuitive resources in quantum optics, is central in physical processes that surpass classical limits. Entanglement between quantum emitters is necessary to perform nonclassical information processing¹ and to go beyond the standard sensitivity limits in interferometry.² Nonclassicality can also be encountered in squeezed states of light,³ where it manifests itself in the reduced quantum fluctuations of the electromagnetic field below the shot-noise level that provide the key to the realization of quantum-enhanced applications in communication, spectroscopy,⁴ and imaging.⁵ The close connection between different manifestations of quantum correlations, such as entanglement and squeezed states in spin-ensembles,² also opens interesting questions regarding the transfer of entanglement in matter to squeezing in light^{6,7} in order to share its nonclassical properties for quantum applications.⁸ Despite extensive studies of the creation of entanglement between emitters by means of continuous-wave squeezed light,^{9,10} the possibility to characterize entanglement via the detection of squeezed light remains widely unexplored.

So far, the emission of squeezed light in resonance fluorescence^{11,12} and the generation of entanglement between quantum emitters¹³ have been demonstrated in a fundamental manner, mainly in free space or microcavities.¹⁰ Recently, there is a strong interest in exploring these quantum effects in new regimes in the coupling strength between matter and light by bringing emitters to integrated nanophotonic systems.^{14,15} The strength of nanostructures relies on their ability to modify both the electromagnetic near and far field, which allows for enhancing and controlling the interaction between emitters.^{14,16}

Several schemes for such nanostructure-mediated coupling have been suggested for the generation of steady-state entanglement between quantum emitters,^{15,17–21} whereas only recently a single emitter source of squeezed light has been proposed.²² Such hybrid environments constitute a suitable platform for enhanced generation of quadrature-squeezed light from a single solid-state emitter, using the techniques recently demonstrated in free space,²³ and it opens the possibility to explore the generation of squeezed light from entangled emitters at the nanoscale. At present, the experimental observation of entanglement in nanophotonic systems remains elusive. One remaining difficulty is that most of the proposed mechanisms rely on either interference arising in detection with low generation probabilities²⁰ or the availability of almost identical emitters.^{17–19} The latter is notoriously difficult in common solid-state emitters, as local properties of the host matrix inhomogeneously distribute the optical transitions, typically by several GHz.^{24–26} These lie outside the reach of narrowband cavities and thus require sophisticated tuning methods.

In this Letter we show how broadband nanostructures assist in the generation of squeezed light arising from the deterministic entanglement of two far-detuned emitters. We identify the connection of the steady-state entanglement between the emitters and the reduced light fluctuations in cooperative resonance fluorescence assisted by nanoarchitectures. Our scheme is based on a two-photon process in a

Received: October 13, 2015

Published: November 18, 2015

coupled pair of two-level emitters with transition frequencies detuned by many line widths ($\omega_2 - \omega_1 = \delta \gg \gamma$). In broadband environments, the single-emitter levels can still be hybridized due to the dipole–dipole coupling potential $\hbar\Omega_{12}$, which arises from the scattering of photons between the emitters and is present even at off-resonant driving as long as $\omega_1, \omega_2 \gg |\delta|$ and the frequency response of the environment varies slowly over $|\delta|$.^{10,16} The resulting collective four-level scheme is depicted in Figure 1a. Two-photon transitions from the fundamental state

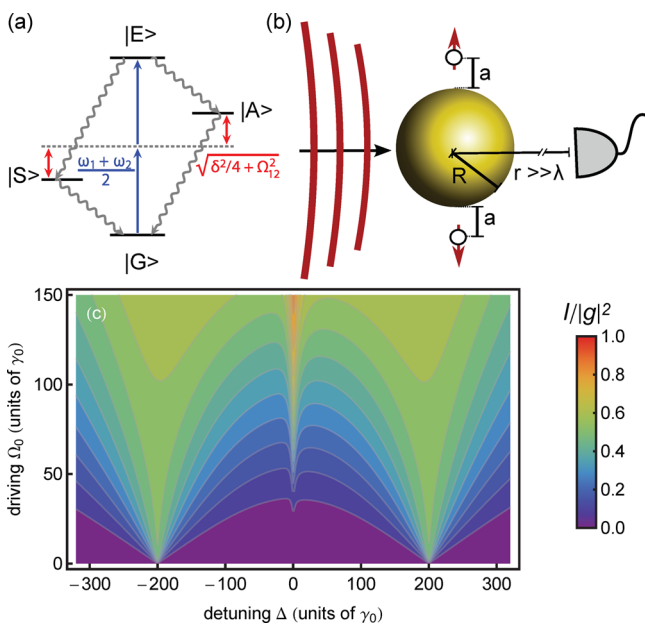


Figure 1. (a) Level scheme of the coupled system, consisting of the fundamental state $|G\rangle = |g_1g_2\rangle$ and doubly excited state $|E\rangle = |e_1e_2\rangle$, connected by a nonlinear two-photon process $\Delta = \omega_L - (\omega_1 + \omega_2)/2 = 0$ (blue arrow), where e_i (g_i) denotes the i th emitter in the excited (ground) state. Due to the emitter detuning δ and coupling Ω_{12} , the dark and bright $|A\rangle$ and $|S\rangle$ (superpositions of single-excitation states $|e_1g_2\rangle, |g_1e_2\rangle$) are nondegenerate. (b) Schematic setup consisting of a pair of two-level dipole emitters coupled to a nanoantenna and illuminated by a coherent driving field. The observation takes place in the far field. (c) Incoherent fluorescence signal as a function of the driving field detuning Δ and free-space Rabi frequency Ω_0 for a configuration of two detuned emitters at a distance $a = 25$ nm from an $R = 40$ nm gold nanosphere ($\lambda = 780$ nm, $\delta = 400\gamma_0$, $\Omega_{12} = -6.4\gamma_0$, $\gamma_{12} = -2.6\gamma_0$, $\gamma = 2.9\gamma_0$), which accounts for the driving field enhancement ($\Omega \approx 2\Omega_0$).

$|G\rangle$ to the doubly excited state $|E\rangle$ at the midfrequency $(\omega_1 + \omega_2)/2$ (blue arrows) become allowed as a result of the dipole–dipole coupling. For emitters coupled by the extreme near field in a bulk medium,²⁷ the incoherent regime of such nonlinear transitions has been verified experimentally.²⁴ Here, we exploit the coherent regime of the transition assisted by a broadband nanostructure that allows generating both squeezed light and entanglement. This is possible when Ω_{12} becomes comparable to the emitters' decay rate γ and when the driving fields, characterized by the Rabi frequency Ω and the laser detuning $\Delta = \omega_L - (\omega_1 + \omega_2)/2$, are weak. The coherence, however, degrades in stronger fields, when the doubly excited state is populated via collective transitions ($\propto \Omega^4\Omega_{12}$) or—to a lesser extent—single-photon transitions ($\propto \Omega^4\Delta$).²⁷ State-of-the-art subwavelength broadband cavities,²⁸ nanowaveguides,^{14,25} or antenna structures¹⁵ can enhance the dipole–dipole cou-

pling^{17,29} outside the extreme near-field regime of bulk environments. All these hybrid systems can overcome saturation broadening and permit much larger emitter separations or even far-field coupling. We find that the nanostructure-assisted nonlinearity allows for the generation of entanglement and the collective emission of squeezed light, necessary to exceed the performance of uncoupled emitters.

As a proof of principle, we consider the system depicted in Figure 1b, consisting of two quantum emitters placed at a distance $a = 25$ nm from a subwavelength gold nanosphere of radius $R = 40$ nm, radially aligned and symmetrically driven. Each of the emitters ($i = 1, 2$) is characterized by the coherence operator of a two-level emitter, $\hat{\sigma}_i = |g\rangle\langle e|$ with resonance frequencies separated by $\delta = 400\gamma_0$. The dynamics of the hybrid system is described by the master equation^{10,16}

$$\dot{\rho} = -\frac{i}{\hbar}[H, \rho] - \sum_{i,j=1,2} \frac{\gamma_{ij}}{2} (\sigma_i^\dagger \sigma_j \rho + \rho \sigma_i^\dagger \sigma_j - 2\sigma_j \rho \sigma_i^\dagger) \quad (1)$$

$$H = \sum_{i=1,2} \hbar(\omega_i - \omega_L) \sigma_i^\dagger \sigma_i - \sum_{i=1,2} \left(\frac{\hbar\Omega_i}{2} \sigma_i^\dagger + \text{H.c.} \right) - \Omega_{12} \sigma_1^\dagger \sigma_2 - \Omega_{12} \sigma_2^\dagger \sigma_1 \quad (2)$$

where H.c. denotes Hermitian conjugate. The scattering by the nanostructure modifies all the coupling constants, including the dipole–dipole coupling Ω_{12} , the incoherent coupling rate γ_{12} , the emitter line width γ , and the Rabi frequency Ω_i , which also contain a contribution from free space ($\Omega_{12,0}$, $\gamma_{12,0}$, γ_0 , and Ω_0 , respectively). This modification allows increasing the bandwidth of the interaction and requires lower driving powers. These coefficients and the positive frequency fields $\vec{E}_i^+ = \mathbf{g}_i \hat{\sigma}_i$, scattered by each of the emitters to the far field mediated by the nanostructure, can be expressed in terms of the full Green's tensor, which describes the full electromagnetic response of both the nanostructure and the surrounding free space and fully encodes the dissipation arising from the material properties. For a gold nanosphere, we evaluate the Green's function semianalytically, using tabulated optical data for gold, and obtain the steady-state correlations of the total scattered field by solving eq 1 (see further details in the Supporting Information). A limit is set by significant nonradiative channels in the decay rates (quenching) and absorption, which degrades the effect of Ω_{12} but can be avoided at distances $a > 10$ nm and wavelengths detuned from the plasmon resonance (see Supporting Information for details). Beyond the example considered here, the formalism and effects are directly transferable to diverse nanophotonic environments,^{14,15} where the dipole–dipole coupling can be further enhanced. Also note that the coupling constants scale with γ_0 , which allows the description of the dynamics for any two-level emitter.

Since the coherent dynamics are limited by the population of the excited states, we first characterize the response to the driving field in terms of the incoherent fluorescence signal $I = \sum_i \langle \vec{E}_i^- \cdot \vec{E}_i^+ \rangle$, which is a common experimental measure of the excitation spectrum and allows identifying the dipole–dipole coupling.²⁴ For relatively equivalent positions of the emitters and a balanced detector position, which should be feasible in state-of-the-art fabrication techniques,^{14,15} we may assume equal scattering amplitudes, Rabi frequencies $\Omega = \Omega_i$, and decay rates $\gamma_i = \gamma$ (the impact of asymmetric configurations is discussed in the Supporting Information). Figure 1c displays

the incoherent fluorescence as a function of the laser detuning Δ and the free-space driving amplitude Ω_0 . Its onset suggests a rough boundary of the coherent regime. Apart from the single-photon resonances at $\Delta \approx \pm\sqrt{(\delta/2)^2 + \Omega_{12}^2}$, there is a clear nonlinear absorption peak at $\Delta = 0$ that arises from the direct two-photon transition from the fundamental state $|G\rangle$ to the doubly excited state $|E\rangle$. The peak saturates for stronger driving Ω , where it eventually overlaps with the saturation-broadened single-emitter lines. The collective fluorescence peak at $\Delta = 0$ would not be observable at comparable emitter separations and detuning in free space since the required stronger excitation field would mainly increase the single-emitter background. Moreover, the intensity observed in the far field ($\propto |g|^2$) is enhanced by a factor of ~ 1.7 with respect to free space,²² and it can still be significantly improved in engineered structures.^{15,30} We finally notice that the large emitter detuning considered here would usually lie outside the interaction range of solid-state emitters in ultrahigh- Q cavities. For example, for cryogenic molecules with typical optical line widths $\gamma_0/2\pi \approx 50$ MHz,²⁴ the equivalent detuning $\delta/2\pi = 20$ GHz would barely lie within the bandwidth of a cavity of $Q = 10^4$.

The coherent excitation via the nanostructure-assisted dipole–dipole interaction makes it possible to generate steady-state entanglement between the two emitters despite their large detuning. We identify bipartite entanglement in the following by nonzero values of the concurrence C , which ranges between 0 for fully separable states and 1 for maximally entangled states.³¹ Figure 2 shows an evaluation of the steady-

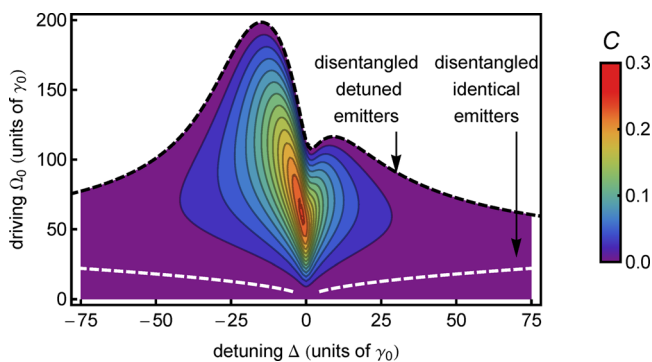


Figure 2. Steady-state concurrence as a function of the driving field amplitude and detuning. Parameters are as in Figure 1. Bipartite entanglement is excluded in the white area for detuned emitters ($\Delta > \Omega_{12}$) and is restricted to the region below the white dashed curve for identical emitters ($\Delta \ll \Omega_{12}$).

state concurrence as a function of the driving field detuning and amplitude for the previous configuration. A significant amount of entanglement can be reached close to the two-photon resonance. As Ω is increased, the onset of saturation in the collective transition shifts this maximum in frequency (asymmetrically due to unequal populations of the entangled states $|A\rangle$ and $|S\rangle$) and finally suppresses entanglement. This behavior differs strongly from the case of identical emitters ($\delta \ll \Omega, \gamma$), for which single-emitter saturation suppresses the generation of entanglement at comparable driving Ω (in the region above the dashed white curve in Figure 2). Moreover, the maximum concurrence $C \approx 0.3$ is comparable to typical values for identical emitters coupled by nanowaveguides via a single-photon process,¹⁷ although concurrence values close to unity

could be achieved by engineered nanostructures with negligible quenching and $\gamma_{12}/\gamma \approx 1$.²¹

Quantum correlations between the emitters^{6,10,32} strongly affect the statistical properties of the scattered light. These can enhance squeezed resonance fluorescence³³ that is characterized by quadrature fluctuations below the shot-noise limit and can be experimentally addressed in homodyne or heterodyne setups.^{3,22} For a general electric field quadrature $\hat{E}_\theta = \sum_i e^{i\theta} \hat{E}_i^\dagger + \text{H.c.}$, we identify reduced fluctuations of a single vector component by a negative value of the normally ordered variance

$$\begin{aligned} (\Delta\mathcal{E})^2 &= \langle : (\hat{E}_\theta - \langle \hat{E}_\theta \rangle)^2 : \rangle \\ &= (\Delta\mathcal{E}_1)^2 + (\Delta\mathcal{E}_2)^2 + (\Delta\mathcal{E}_{12})^2. \end{aligned}$$

Here, the fluctuations from single emitters correspond to

$$\frac{(\Delta\mathcal{E}_i)^2}{2|g_i|^2} = (\langle \hat{\sigma}_i^\dagger \hat{\sigma}_i \rangle - |\langle \hat{\sigma}_i \rangle|^2) - \text{Re}[e^{2i(\theta+\phi_i)} \langle \hat{\sigma}_i \rangle^2] \quad (3)$$

with scattering phases $\phi_i = \arg(g_i)$ and recover previous results²² in the absence of coupling between the emitters. The interaction modifies each of these terms and gives rise to the additional cross-correlations

$$\begin{aligned} \frac{(\Delta\mathcal{E}_{12})^2}{2|g_1 g_2|} &= 2\text{Re}[e^{i(\phi_1 - \phi_2)} (\langle \hat{\sigma}_2^\dagger \hat{\sigma}_1 \rangle - \langle \hat{\sigma}_2^\dagger \rangle \langle \hat{\sigma}_1 \rangle) \\ &\quad + e^{i(2\theta + \phi_1 + \phi_2)} (\langle \hat{\sigma}_2 \hat{\sigma}_1 \rangle - \langle \hat{\sigma}_2 \rangle \langle \hat{\sigma}_1 \rangle)] \end{aligned} \quad (4)$$

that clearly vanish for uncorrelated emitters. Therefore, negative values arising from the cross-terms denote reduced fluctuations that allow identifying bipartite entanglement.

The black curve in Figure 3a shows the optimum degree of squeezing $(\Delta\mathcal{E})^2/2|g|^2$, obtained by varying the phases θ and ϕ_i , as a function of the laser detuning. The driving $\Omega_0 = 60\gamma_0$ was chosen well below the two-photon saturation. As before, we focus on a favorable balanced detection configuration ($|g_1| = |g_2|$; see Supporting Information for a discussion of the general case). A distinct minimum of the fluctuations arises close to the two-photon resonance $\Delta = 0$ and mirrors the behavior of the concurrence, indicated by the red (upper) curve. To exemplify the link between entanglement in matter and squeezing in light and to understand the main mechanism underlying the present scheme, we consider a simplified model for weak driving on the two-photon resonance. An effective two-level picture arises because the single-photon transitions are far detuned and the dipole–dipole coupling mainly induces a coherence ρ_{EG} between the fundamental and doubly excited state, so that the density matrix is dominated by this element and the populations. From these elements, we find from eqs 3 and 4 the normalized degree of squeezing

$$\frac{(\Delta\mathcal{E})^2}{2|g|^2} \approx 1 - \rho_{GG} + \rho_{EE} + \text{Re}[e^{i(\theta + \phi_1 + \phi_2)} \rho_{EG}] \quad (5)$$

which is optimized when the last term equals $-\rho_{EG}$. The approximation (green dash-dotted curve) agrees excellently with the full squeezing amplitude (black curve). Interestingly, eq 5 is closely related to the spin squeezing^{2,9} present in the system and reinforces the link to entanglement. In fact, a similar treatment of the concurrence near the resonance (blue dashed line) is equally dominated by $|\rho_{EG}|$ (see Supporting Information for details). Altogether this identifies the two-photon coherence

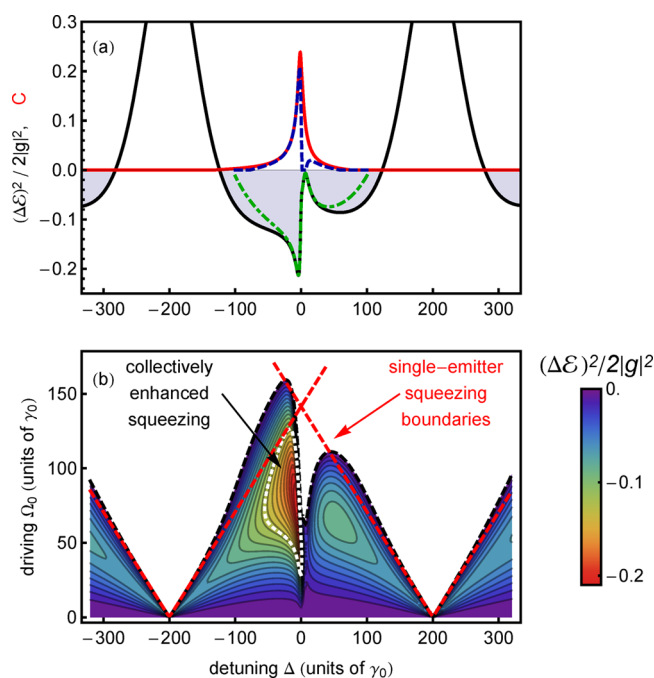


Figure 3. (a) Electric field fluctuations (black curve) obtained by optimizing the detection quadrature angle and steady-state concurrence (red curve) vs laser detuning at $\Omega_0 = 60\gamma_0$. The gray shading indicates squeezed light. The green and blue dashed curves give the effective two-level approximation on the $|E\rangle - |G\rangle$ transition for the squeezing and the concurrence, respectively. (b) Electric field fluctuations as a function of the driving field detuning and amplitude, optimizing the detection quadrature angle. No squeezing can be observed above the black dashed limit. The red curves indicate the limits for independent emitters. The fluctuations exceed the minimum value feasible from two independent emitters inside the white contour. Parameters are chosen as in Figure 1.

as the source of both squeezing and entanglement and supports the description in terms of an effective two-level model.

A full evaluation of the electric field fluctuations as a function of the driving field amplitude and detuning is given in Figure 3b. At the chosen parameters, the strongest squeezing is encountered at $\Omega_0 \approx 75\gamma_0$ near the center frequency $\Delta \approx 0$ and closely follows the regime that allows for maximum bipartite entanglement in Figure 2. When the driving field intensity is further increased, saturation of the two-photon transition suppresses squeezing at $\Delta = 0$, similar to the concurrence. As the collective interaction also affects eq 3, the boundaries of squeezed light can surpass the ones for uncoupled emitters²² (denoted by the red dashed limits in Figure 3b). The strongest squeezing with values $(\Delta\mathcal{E})^2/(2|g|^2) \approx -0.21$ significantly exceeds the universal threshold -0.125 that limits the squeezed resonance fluorescence from independent emitters²² and is indicated by the white contour in Figure 3b. Thus, a strong collective enhancement of the squeezing per emitter³³ can be achieved despite their large detuning. This is a general result for pairs of two-level systems coupled by means of strong dipole–dipole interactions and can be used to identify entanglement.

As an advantage for the realization of nanoscopic sources of squeezed light, the collective effects induced by the nanoarchitecture allow for overcoming significant additional pure dephasing (see further details in the Supporting Information). This phenomenon occurs commonly in solid-state environments due to the coupling to thermal phonons, and it presents

a main limitation to the operation time of quantum gates. For independent emitters, additional pure dephasing at a rate $\gamma^* \geq \gamma/2$ will fully suppress the generation of squeezed light, even though the enhancing effect of a nanostructure may modify the boundary significantly.²² At the onset of this unfavorable scenario, we represent in Figure 4 the minimized electric field

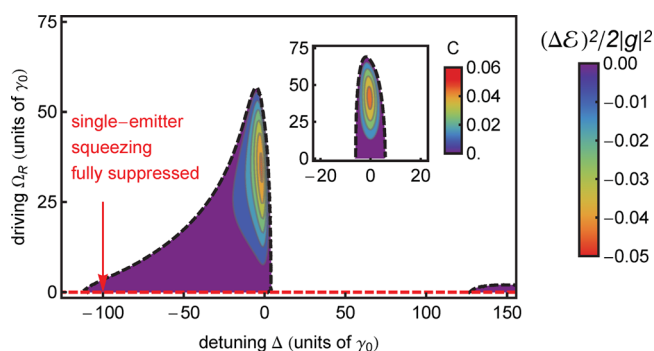


Figure 4. Maximum degree of squeezing as a function of the driving field detuning and amplitude, obtained by optimizing the detection quadrature angle in the presence of strong additional pure dephasing processes at a rate $\gamma^* = 2\gamma$, for which single-emitter squeezing is fully suppressed (cf. red dashed limit). All other parameters are as in Figure 1. Inset: Analogous representation for the concurrence.

fluctuations as a function of the driving field and detuning. The full suppression of squeezing for uncoupled emitters is indicated by the red dashed limit, i.e., $(\Delta\mathcal{E})^2 \geq 0$ for all Ω_0 . Still, a significant amount of squeezing survives near the two-photon resonance, although at a reduced absolute value. The optimum follows even more closely the behavior of the concurrence (shown in the inset) than in the absence of pure dephasing because terms stemming from the single emitters are now suppressed. These facts reflect that squeezed emission identifies entanglement despite additional dephasing and underline that nanostructures allow tailoring collective interactions, providing more robust sources of squeezed light in the presence of decoherence.

The combination of nanophotonic structures with quantum emitters presents promising prospects for novel integrated collective sources of squeezed light and the generation of multipartite entanglement at the nanoscale. We have shown that a metallic nanosphere, as a fundamental example, can mediate a two-photon process that leads to both entanglement and squeezing for two emitters with nonoverlapping transitions. This can greatly relax the requirement of tuning the optical resonances of solid-state emitters to achieve large degrees of entanglement in hybrid systems. Moreover, we have shown that the collective generation of squeezed light from two interacting quantum emitters assisted by the nanostructure can surpass the limiting squeezing level of independent emitters and can provide a reliable witness of entanglement. Therefore, resonance fluorescence from interacting emitters can help to explore the transfer of nonclassicality from matter to light in nanophotonic devices that surpasses the limits of classical optics.^{2,8} The nanostructure-assisted collective interaction in our scheme helps to overcome a significant amount of additional pure dephasing, even beyond the constraints on uncoupled emitters.²² As both nanophotonic enhancement and collectivity counteract phase decoherence—a fundamental limit in setups at nonzero temperatures—nanostructures can help to scale up the operating temperatures of solid-state emitters. A

simple estimation for typical molecules³⁴ shows that an increase of 300 in the radiative line width could allow working at temperatures of ~ 70 K rather than below 5 K, with possible technological implications. Our results can be transferred to other broadband environments such as optical antennas, subwavelength cavities, or nanowaveguides, to push further the limits for generating squeezed light. Suitable quantum-emitter frameworks can be realized by promising emerging techniques based on the deterministic positioning of self-assembled quantum dots close to these nanophotonic structures¹⁴ or by scanning a nanostructured probe over a spin-coated layer of emitters.¹⁵ We expect that these collective effects may be scaled up to higher numbers of emitters,^{18,19,35} a study of which can provide a better understanding of squeezing in structured nonlinear media.

■ ASSOCIATED CONTENT

● Supporting Information

The Supporting Information is available free of charge on the ACS Publications website at DOI: 10.1021/acsp Photonics.5b00585.

Detailed description of the master equation and Green's tensor calculation. Dipole–dipole coupling and quenching parameter dependence. Impact of asymmetric coupling scenarios. Asymptotic evaluation of the concurrence and quadrature fluctuations. Connection to spin squeezing (PDF)

■ AUTHOR INFORMATION

Corresponding Authors

*E-mail: harald.haakh@mpl.mpg.de.

*E-mail: diego-martin.cano@mpl.mpg.de.

Notes

The authors declare no competing financial interest.

■ ACKNOWLEDGMENTS

Financial support from the Max Planck Society is gratefully acknowledged. We thank A. Maser, B. Gmeiner, S. Götzinger, A. González-Tudela, M. Agio, and V. Sandoghdar for helpful discussions.

■ REFERENCES

- (1) Bremner, M.; Dawson, C.; Dodd, J.; Gilchrist, A.; Harrow, A.; Mortimer, D.; Nielsen, M.; Osborne, T. Practical scheme for quantum computation with any two-qubit entangling gate. *Phys. Rev. Lett.* **2002**, *89*, 247902.
- (2) Pezzé, L.; Smerzi, A. Entanglement, nonlinear dynamics, and the Heisenberg limit. *Phys. Rev. Lett.* **2009**, *102*, 100401.
- (3) Loudon, R.; Knight, P. L. Squeezed light. *J. Mod. Opt.* **1987**, *34*, 709–759.
- (4) Drummond, P. D.; Ficek, Z., Eds. *Quantum Squeezing*; Springer-Verlag: Berlin, Heidelberg, 2010.
- (5) Taylor, M. A.; Bowen, W. P. Quantum metrology and its application in biology. *eprint* 2014, arXiv:1409.0950.
- (6) Saito, H.; Ueda, M. Quantum-controlled few-photon state generated by squeezed atoms. *Phys. Rev. Lett.* **1997**, *79*, 3869.
- (7) Grünwald, P.; Vogel, W. Quantum-entangled light from localized emitters. *Phys. Rev. A: At, Mol., Opt. Phys.* **2014**, *90*, 022334.
- (8) Meyer, V.; Rowe, M. A.; Kielpinski, D.; Sackett, C. A.; Itano, W. M.; Monroe, C.; Wineland, D. J. Experimental Demonstration of Entanglement-Enhanced Rotation Angle Estimation Using Trapped Ions. *Phys. Rev. Lett.* **2001**, *86*, 5870–5873.
- (9) Hammerer, K.; Sørensen, A. S.; Polzik, E. S. Quantum interface between light and atomic ensembles. *Rev. Mod. Phys.* **2010**, *82*, 1041.
- (10) Ficek, Z.; Tanas, R. Entangled states and collective nonclassical effects in two-atom systems. *Phys. Rep.* **2002**, *372*, 369–443.
- (11) Lu, Z.; Bali, S.; Thomas, J. Observation of squeezing in the phase-dependent fluorescence spectra of two-level atoms. *Phys. Rev. Lett.* **1998**, *81*, 3635.
- (12) Ourjoumtsev, A.; Kubanek, A.; Koch, M.; Sames, C.; Pinkse, P. W.; Rempe, G.; Murr, K. Observation of squeezed light from one atom excited with two photons. *Nature* **2011**, *474*, 623–626.
- (13) Hagley, E.; Maitre, X.; Nogues, G.; Wunderlich, C.; Brune, M.; Raimond, J.-M.; Haroche, S. Generation of Einstein-Podolsky-Rosen pairs of atoms. *Phys. Rev. Lett.* **1997**, *79*, 1.
- (14) Lodahl, P.; Mahmoodian, S.; Stobbe, S. Interfacing single photons and single quantum dots with photonic nanostructures. *Rev. Mod. Phys.* **2015**, *87*, 347–400.
- (15) Tame, M.; McEnery, K.; Özdemir, Ş.; Lee, J.; Maier, S.; Kim, M. Quantum plasmonics. *Nat. Phys.* **2013**, *9*, 329–340.
- (16) Dung, H. T.; Knöll, L.; Welsch, D.-G. Resonant dipole-dipole interaction in the presence of dispersing and absorbing surroundings. *Phys. Rev. A: At, Mol., Opt. Phys.* **2002**, *66*, 063810.
- (17) González-Tudela, A.; Martín-Cano, D.; Moreno, E.; Martín-Moreno, L.; Tejedor, C.; García-Vidal, F. J. Entanglement of Two Qubits Mediated by One-Dimensional Plasmonic Waveguides. *Phys. Rev. Lett.* **2011**, *106*, 020501.
- (18) Gullans, M.; Tiecke, T. G.; Chang, D. E.; Feist, J.; Thompson, J. D.; Cirac, J. I.; Zoller, P.; Lukin, M. D. Nanoplasmonic Lattices for Ultracold Atoms. *Phys. Rev. Lett.* **2012**, *109*, 235309.
- (19) González-Tudela, A.; Porras, D. Mesoscopic entanglement induced by spontaneous emission in solid-state quantum optics. *Phys. Rev. Lett.* **2013**, *110*, 080502.
- (20) Lee, C.; Tame, M.; Noh, C.; Lim, J.; Maier, S. A.; Lee, J.; Angelakis, D. G. Robust-to-loss entanglement generation using a quantum plasmonic nanoparticle array. *New J. Phys.* **2013**, *15*, 083017.
- (21) Hou, J.; Slowik, K.; Lederer, F.; Rockstuhl, C. Dissipation-driven entanglement between qubits mediated by plasmonic nanoantennas. *Phys. Rev. B: Condens. Matter Mater. Phys.* **2014**, *89*, 235413.
- (22) Martín-Cano, D.; Haakh, H. R.; Murr, K.; Agio, M. Large Suppression of Quantum Fluctuations of Light from a Single Emitter by an Optical Nanostructure. *Phys. Rev. Lett.* **2014**, *113*, 263605.
- (23) Schulte, C. H.; Hansom, J.; Jones, A. E.; Matthiesen, C.; Gall, C. L.; Atature, M. Quadrature squeezed photons from a two-level system. *Nature* **2015**, *525*, 222–225.
- (24) Hettich, C.; Schmitt, C.; Zitzmann, J.; Kühn, S.; Gerhardt, I.; Sandoghdar, V. Nanometer resolution and coherent optical dipole coupling of two individual molecules. *Science* **2002**, *298*, 385–389.
- (25) Faez, S.; Türschmann, P.; Haakh, H. R.; Götzinger, S.; Sandoghdar, V. Coherent Interaction of Light and Single Molecules in a Dielectric Nanoguide. *Phys. Rev. Lett.* **2014**, *113*, 213601.
- (26) Patel, R. B.; Bennett, A. J.; Farrer, I.; Nicoll, C. A.; Ritchie, D. A.; Shields, A. J. Two-photon interference of the emission from electrically tunable remote quantum dots. *Nat. Photonics* **2010**, *4*, 632–635.
- (27) Varada, G. V.; Agarwal, G. S. Two-photon resonance induced by the dipole-dipole interaction. *Phys. Rev. A: At, Mol., Opt. Phys.* **1992**, *45*, 6721–6729.
- (28) Kelkar, H.; Wang, D.; Martín-Cano, D.; Hoffmann, B.; Christiansen, S.; Götzinger, S.; Sandoghdar, V. A Sub- λ^3 Volume Cantilever-based Fabry-Pérot Cavity. *Phys. Rev. Appl.* **2015**, *4*, 054010.
- (29) Agarwal, G. S.; Gupta, S. D. Microcavity-induced modification of the dipole-dipole interaction. *Phys. Rev. A: At, Mol., Opt. Phys.* **1998**, *57*, 667.
- (30) Rogobete, L.; Kaminski, F.; Agio, M.; Sandoghdar, V. Design of plasmonic nanoantennae for enhancing spontaneous emission. *Opt. Lett.* **2007**, *32*, 1623–1625.
- (31) Wootters, W. K. Entanglement of Formation of an Arbitrary State of Two Qubits. *Phys. Rev. Lett.* **1998**, *80*, 2245–2248.
- (32) Tanaš, R.; Ficek, Z. Entanglement of two atoms. *Fortschr. Phys.* **2003**, *51*, 230–235.
- (33) Ficek, Z.; Tanas, R. Squeezing in two-atom resonance fluorescence induced by two-photon coherences. *Quantum Opt.* **1994**, *6*, 95–106.

(34) Irngartinger, T.; Bach, H.; Renn, A.; Wild, U. P. *Electrical and Related Properties of Organic Solids*; Springer, 1997; pp 359–367.

(35) Delga, A.; Feist, J.; Bravo-Abad, J.; Garcia-Vidal, F. Quantum Emitters Near a Metal Nanoparticle: Strong Coupling and Quenching. *Phys. Rev. Lett.* **2014**, *112*, 253601.